

## La<sub>2</sub>O<sub>3</sub>-encapsulated-SnO<sub>2</sub> nanocrystallite-based photoanodes for enhanced DSSCs performance

Shoyebmohamad F. Shaikh<sup>a,b</sup>, Rajaram S. Mane<sup>a</sup>, and Oh-Shim Joo<sup>\*a</sup>

### Supporting information

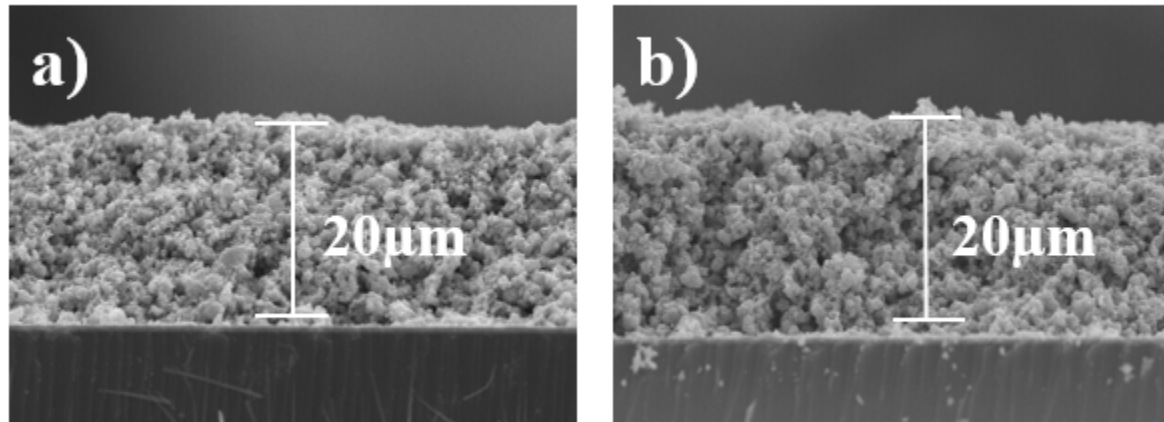


Figure S1: Cross-section images electrodes of; a) SnO<sub>2</sub> and SnO<sub>2</sub>- La<sub>2</sub>O<sub>3</sub> electrodes.

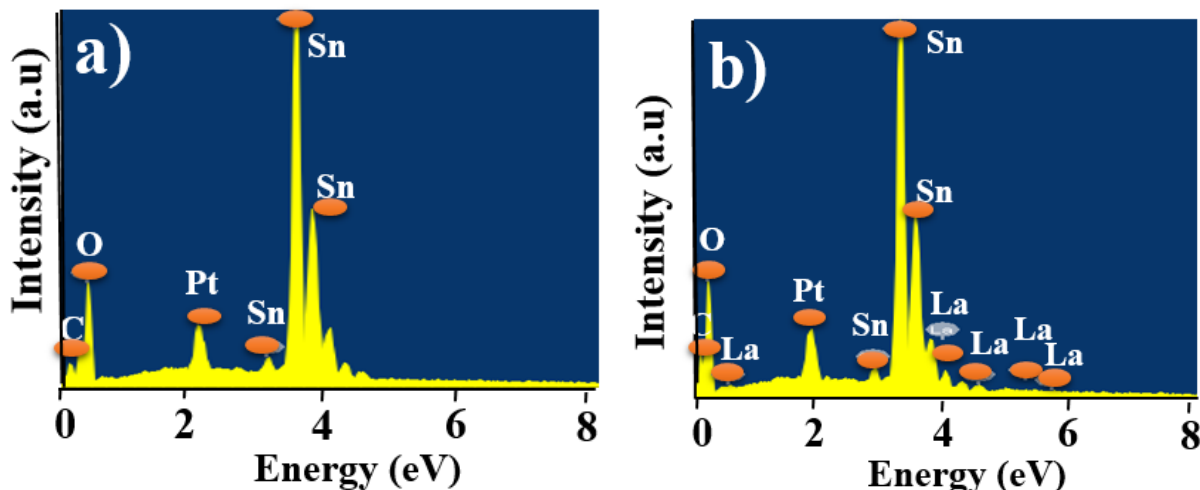
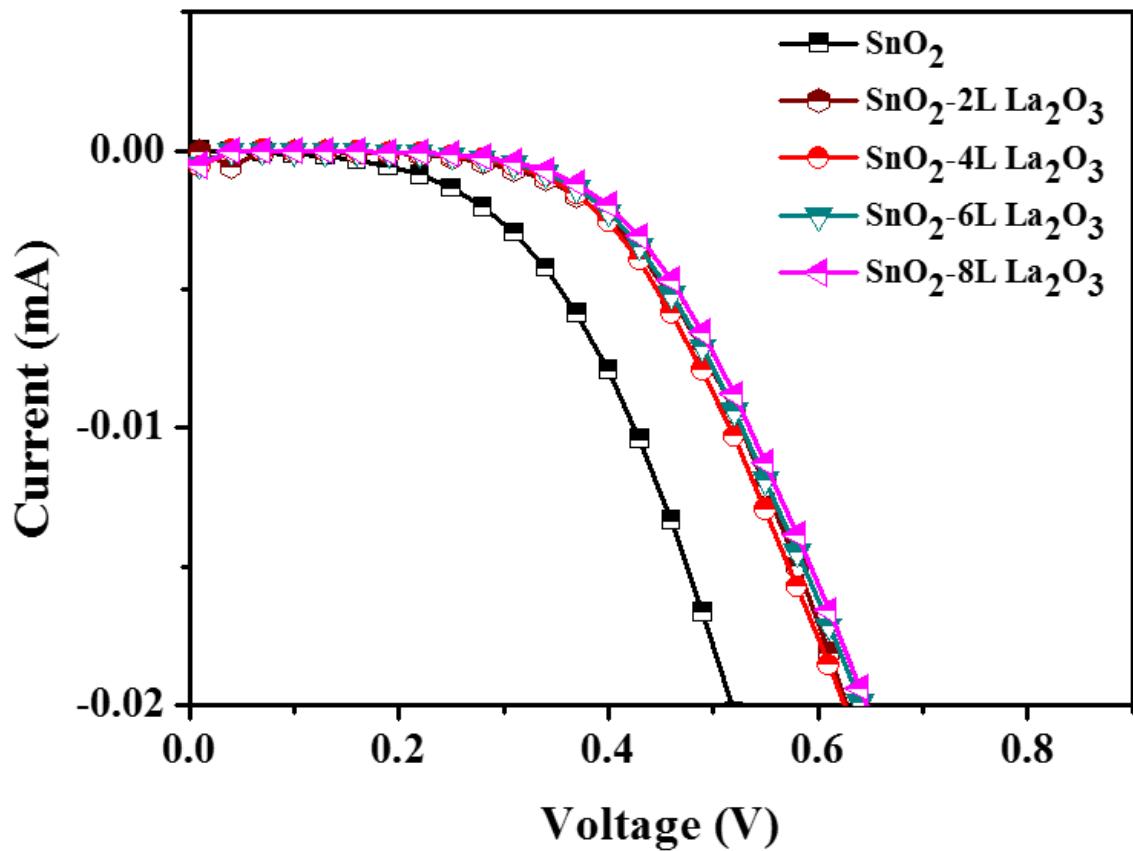
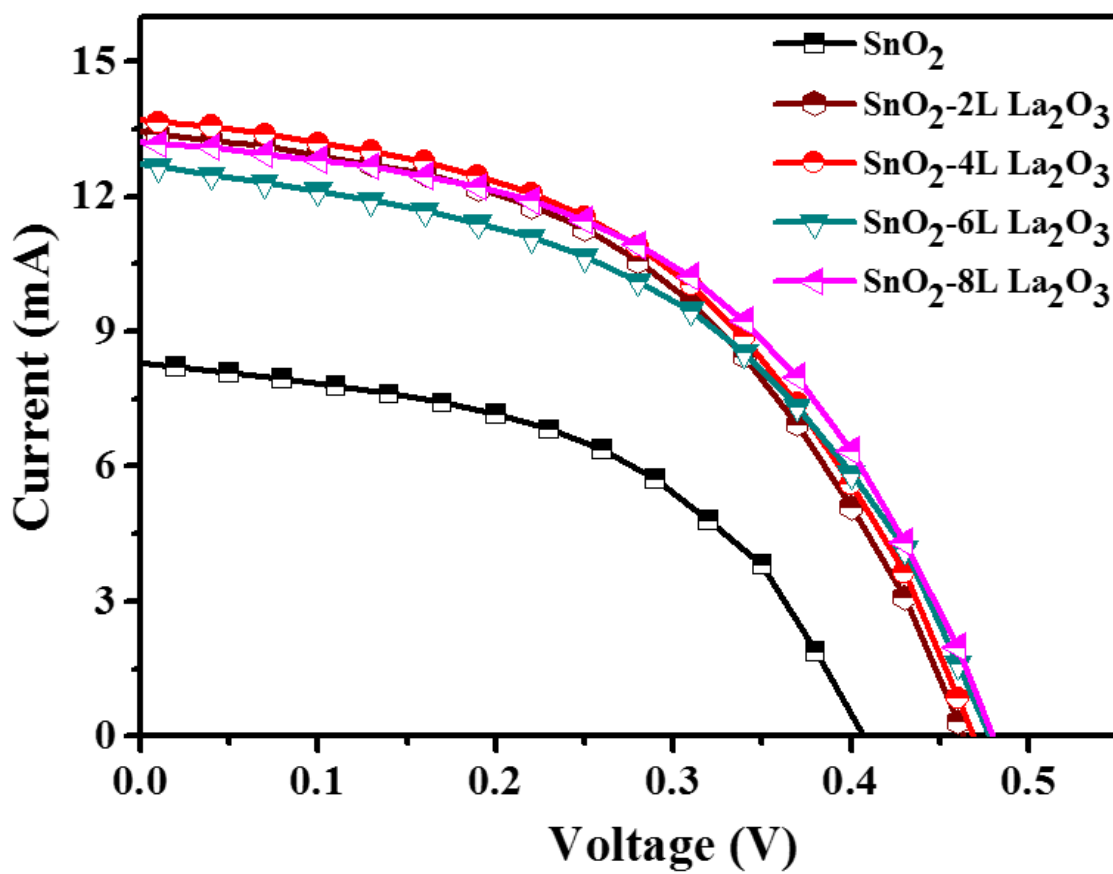


Figure S2: EDX analysis of; a) SnO<sub>2</sub> and SnO<sub>2</sub>- La<sub>2</sub>O<sub>3</sub>. Platinum peak occurrence was unprecedented in present study.



**Figure S3:** Dark Current  $J$ - $V$  plots of SnO<sub>2</sub> and SnO<sub>2</sub>-La<sub>2</sub>O<sub>3</sub> photoanodes under dark as a function spin-coating layer.



**Figure S4-** J-V curves of SnO<sub>2</sub> and SnO<sub>2</sub>-La<sub>2</sub>O<sub>3</sub> photoanodes under light as a function spin-coating layer.

**Table S1:** Change in photovoltaic parameters of SnO<sub>2</sub>-based DSSCs as a function of La<sub>2</sub>O<sub>3</sub> layering number.

Photoanode	J <sub>sc</sub> (mA cm <sup>-2</sup> )	V <sub>oc</sub> (V)	FF	η (%)
SnO <sub>2</sub>	8.30	0.40	0.49	1.66
SnO <sub>2</sub> -2L La <sub>2</sub> O <sub>3</sub>	13.42	0.46	0.48	2.98
SnO <sub>2</sub> -4L La <sub>2</sub> O <sub>3</sub>	13.61	0.46	0.48	3.0
SnO <sub>2</sub> -6L La <sub>2</sub> O <sub>3</sub>	13.21	0.47	0.50	3.0
SnO <sub>2</sub> -8L La <sub>2</sub> O <sub>3</sub>	12.71	0.47	0.48	2.93